

Article

Estimation of the Optimum Tilt Angle of Solar PV Panels to Maximize Incident Solar Radiation in Libya[†]

Alhassan Ali Teyabeen *  and Faisal Mohamed

Libyan Authority of Scientific Research, Tipoli P.O. Box 80045, Libya; elabdli@hotmail.com

* Correspondence: alhassan.teyabeen@gmail.com

[†] This paper is an extended version of our paper published in Proceedings of 2022 13th International Renewable Energy Congress (IREC), Hammamet, Tunisia, 13–15 December 2022; pp. 1–7.

Abstract: The most significant factor affecting the performance of a solar photovoltaic (PV) system is its tilt angle. It determines the amount of incident solar energy at the panel surface. In this paper, the optimum tilt angle of solar PV panels is estimated based on measured data recorded in twelve major cities in Libya by changing the panel's tilt angle from 0° up to 90° in steps of 1° and searching for the corresponding maximum daily total solar radiation. A non-linear regression technique was applied to establish six empirical models to determine the optimum tilt angle in Libya. The accuracy of the models was evaluated using statistical criteria such as Taylor diagrams, root mean square error, mean bias error, and correlation coefficient. The results demonstrated that the monthly optimum tilt angle increased during the winter and decreased during the summer varying from 0° to 59°. In addition, both third-order polynomial and Fourier models presented the best efficiency in estimating the optimum tilt angle with a correlation coefficient of 0.9943. The percent gain in average yearly solar energy received at the monthly optimum tilt angle varies from 12.43% to 17.24% for all studied sites compared to the horizontal surface.

Keywords: photovoltaic systems; solar radiation; optimum tilt angle; statistical analysis; Libya



Citation: Teyabeen, A.A.; Mohamed, F. Estimation of the Optimum Tilt Angle of Solar PV Panels to Maximize Incident Solar Radiation in Libya. *Energies* **2024**, *17*, 5891. <https://doi.org/10.3390/en17235891>

Academic Editor: Carlo Renno

Received: 19 December 2023

Revised: 9 February 2024

Accepted: 1 March 2024

Published: 23 November 2024



Copyright: © 2024 by the authors. Licensee MDPI, Basel, Switzerland. This article is an open access article distributed under the terms and conditions of the Creative Commons Attribution (CC BY) license (<https://creativecommons.org/licenses/by/4.0/>).

1. Introduction

Sunlight is one of the most abundant and inexhaustible renewable sources. Solar photovoltaic systems generate power by the direct conversion of sunlight into electricity, thus they are clean and safe for the environment compared with fossil fuels which cause a significant negative impact on the environment when burned due to the emissions of hazardous gases and carbon dioxide. The amount of incident solar radiation at specified inclined surfaces should be accurately determined before installing solar photovoltaic systems at any location. It is a key input for designing solar PV systems, thus the tilt angle must be properly estimated. Several studies have reported the optimal tilt angles estimation, Obiwulu et al. [1] introduced many models to determine the optimal tilt angle and its corresponding total radiation in 37 Nigerian cities. Three different ways to install six PV panels were selected; horizontal surface, south-facing, and north-facing. The panel which fixed on 16.8° south-facing introduced the best performance for exploiting the maximum incident solar radiation.

Hassan et al. [2] calculated the optimal tilt angle to exploit the highest possible solar radiation capacity in eighteen Iraqi cities. The presented results illustrated that the maximum level of solar radiation was obtained at the angles of inclination of 0°–64°, and that the optimal tilt angle increased during winter and decreased during summer. Jamil [3] estimated the amount of solar radiation for tilted south-facing surfaces in Aligarh and New Delhi in India. The annual, seasonal, and monthly optimum tilt angles were also estimated. For better performance of solar energy systems, the percentage gains in annual mean solar radiation were calculated based on the determinate annual optimum tilt angle. The values

were 6.51% and 7.58% for Aligarh and New Delhi, respectively. The study recommended that the tilted surfaces in the studied sites must be set on monthly or seasonal optimum tilt angles for better capturing of solar radiation. Mansour et al. [4] determined the optimal annual and monthly tilt angles of photovoltaic modules to increase the output power of photovoltaic systems in different locations in Saudi Arabia. The study also achieved the influence of ambient temperature on the photovoltaic systems performance. As a case study, a solar power generation system with a nominal output of 2.76 kWp is utilized for evaluation of its performance. The presented results illustrated that the annual tilt angles ranged between 20.1° to 32.7° for the studied location. The orientation of the module and ambient temperature were the factors found to most affect the performance of photovoltaic systems. Alqaed et al. [5] calculated the ideal tilt angle for solar photovoltaic panel surfaces facing south for the city of Najran—Saudi Arabia using the horizontal solar radiation data. The annual optimum tilt angle for the considered location was found as 20.97°. The average gains in yearly solar radiation based on monthly, seasonal, and yearly optimum tilt angles compared to the horizontal surface were 9.56%, 8.08%, and 3.32%, respectively. Bakirci [6] used the measured global solar radiation data collected in 8 provinces in Turkey to determine the optimal tilt angle by varying the inclined surface of the solar collector from 0° to 90° to exploit the maximum incident solar radiation. The study results illustrated that the monthly optimal tilt angle for the studied sites ranged between 0° and 65°. Furthermore, three different mathematical models were introduced to determine the optimal tilt angle. Their performance was assessed using different statistical criteria such as mean bias error, correlation coefficient, root mean square error, and t-statistic. The third-order polynomial was the most accurate model in determining the optimal tilt angle. Al-Sayyab et al. [7] evaluated the effect of variation of tilt angle on the power generated from the solar photovoltaic panel. The achieved work presented an experimental and simulation study. The study was conducted in the city of Basra. It proposed a mathematical model to find the optimum tilt angle. The model was validated using an experimental test by changing the tilt angle from 0° to 90° with a step of 5°. The results showed that the annual optimum tilt angle is equal to 28°. Baileka et al. [8] investigated the maximization of solar energy incident on the inclined surfaces of PV panels. The results showed that for monthly seasonal semi-annual and yearly adjustments, solar energy increased by 20.61%, 19.58%, 19.24% and 13.78%, respectively. Nanning city in China was selected as a case study to analyze the optimal options for installing solar PV systems and determine the PV energy potential of solar PV. According to the analysis, the annual optimum tilt and azimuth angles were 32° and 245°, respectively. Rooftop photovoltaic projects can generate 19.99 TWh per year, which would meet 76.1% of the city's electricity needs [9]. Kaddoura et al. [10] investigated the optimum tilt angles of PV panels for many cities in the Kingdom of Saudi Arabia based on horizontal solar radiation data obtained from NASA. The results showed that adjusting the tilt angle six times per year provides 99.5% of the solar radiation that can be achieved with daily adjustment of solar PV panels. Despotovic and Nedic [11] determined the optimum tilt angle of solar panels in Belgrade by searching for the best orientation and inclination values that give the total radiation over the given period. Jafarkazemi and Saadabadi [12] evaluated the influence of optimum tilt angle and orientation of solar collectors and solar PV modules in Abu Dhabi based on monthly average daily solar radiation data obtained from NASA. Results demonstrated that the inclined surface should be changed at least twice a year. Chang [13] employed the nonlinear particle swarm method with nonlinear time-varying evolution to determine the optimal tilt angles of solar PV panels in seven selected cities in Taiwan, for maximizing electrical energy from the panels. Khorasanizadeh et al. [14] determined the monthly, seasonal, semi-yearly, and yearly optimum tilt angles for south-facing photovoltaic surfaces in Tabass, Iran. A diffuse solar radiation model from three different categories was established to estimate the optimum tilt angle. From the statistical analysis, the cubic model was recognized as the best. Bojić et al. [15] estimated the optimum azimuth and tilt angle for solar PV systems in four French cities. The results were determined based on one year of experimental solar radiation data. In Athens, Greece,

ref. [16] demonstrated an optimum tilt angle of PV panels in the summer season and found that the angle of $15^\circ (\pm 2.5^\circ)$ is the optimum angle. In Brisbane, Australia, Yan et al. [17] developed a mathematical model to estimate the performance of solar PV systems at different tilt angles. As a result, the optimal inclination and orientation angles were found to be 26° N facing true north. Various other studies have been reported on the field of optimization of tilt angles, they have considered the impact of wind speed cooling [18,19], cloudiness [20], maximizing incident radiation on flat plate collectors [21], maximizing solar radiation on PV surface [22–24], maximizing energy produced by PV panels [25–27]. Other studies used optimization algorithms for determining the optimal tilt angle including particle swarm optimization (PSO) [28,29], artificial neural network (ANN) [30,31] and genetic algorithm (GA) [32,33].

Although several studies have reported on estimating the optimum tilt angle [34–37], their limitations were that the percent loss in solar energy obtained at the surface inclined to the annual optimum tilt angle was not determined. In this study, measured data recorded by real weather stations on the ground at the selected sites were used to estimate the optimum tilt angle. This makes the study results more reliable compared with other studies which used satellite data such as those obtained from NASA and the GIS database [36,37].

The purpose of this study is to:

- Find the best monthly, seasonal, and yearly tilt angles of solar photovoltaic panels to maximize the incident solar radiation.
- Compare the presented results with other published results achieved in the same region.
- Establish empirical models for estimating the optimum tilt angle in twelve major cities in Libya.
- Validate the established models using different statistical criteria.

2. Materials and Methods

2.1. Case Study Regions and Data Resources

The measured global solar radiation data used in this study were collected from twelve meteorological stations (Table 1, and Figure 1) on the ground distributed throughout Libya obtained from the National Center of Meteorology, and the Libyan Center for Solar Energy Research and Studies. The measured meteorological data in the site of Tripoli were collected by the meteorological station shown in Figure 2a during the period of 2018–2020 and recorded every 10 min using the pyranometer type of CMA11 fabricated by KIPP & ZONEN as shown in Figure 2b. It is classified by ISO 6090-1990 classification as secondary standard [38], and has a sensitivity of $8.79 \times 10^{-6} \text{ V/Wm}^{-2}$. The climatic station measures several climatic factors including direct normal, diffused, tilted, and horizontal global solar radiation. It also measures other factors such as UV, pressure, wind speed and direction. The solar radiation data collected in the other studied sites were collected during the period of 1981–1988 and measured by a bimetallic sensor called the “Robitzsch bimetallic actinograph” (Figure 2c). The measuring accuracy is about $\pm 5\%$ [39]. This instrument has been used for measuring solar radiation in various regions around the world [39–44].

Table 1. Information for the studied locations in this study.

| Location | Latitude | Longitude |
|----------|--------------------------|--------------------------|
| Bengazi | $32^\circ 05' \text{ N}$ | $20^\circ 16' \text{ E}$ |
| Ajdabia | $30^\circ 43' \text{ N}$ | $20^\circ 10' \text{ E}$ |
| Jalu | $29^\circ 02' \text{ N}$ | $21^\circ 34' \text{ E}$ |
| Kufra | $24^\circ 14' \text{ N}$ | $23^\circ 18' \text{ E}$ |
| Sebha | $27^\circ 01' \text{ N}$ | $14^\circ 26' \text{ E}$ |
| Hun | $29^\circ 08' \text{ N}$ | $15^\circ 57' \text{ E}$ |

Table 1. Cont.

| Location | Latitude | Longitude |
|-----------|----------|-----------|
| Elgariyat | 30°23' N | 13°35' E |
| Tripoli | 32°48' N | 13°26' E |
| Nalut | 31°52' N | 10°59' E |
| Ghadames | 30°08' N | 9°30' E |
| Ghat | 25°08' N | 10°08' E |
| Sirt | 31°12' N | 16°35' E |

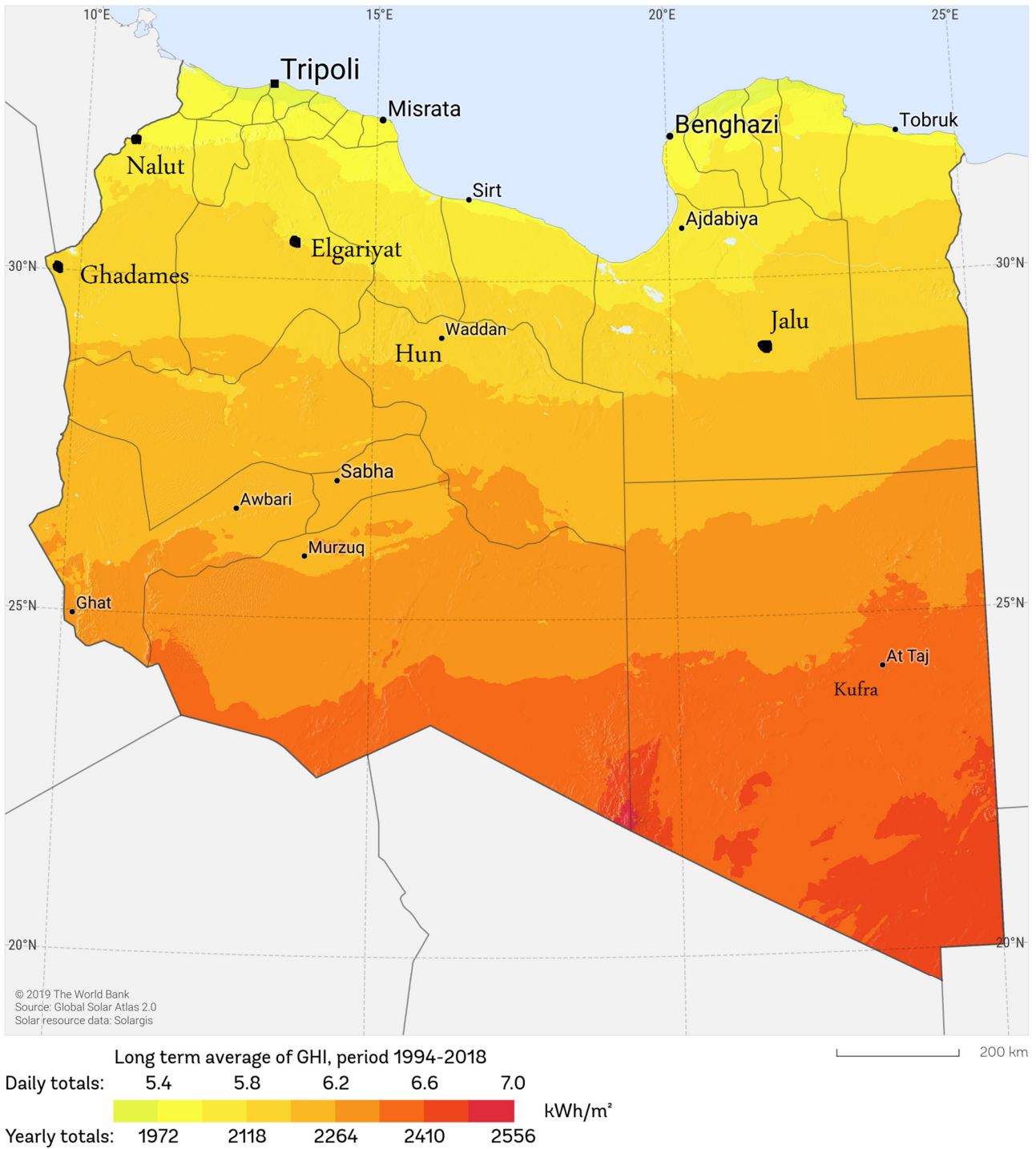


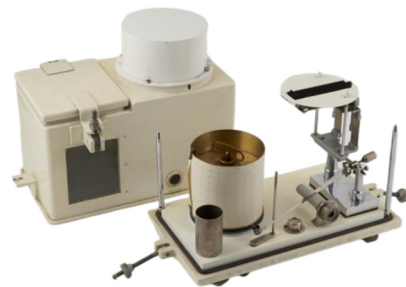
Figure 1. Global solar radiation map of Libya (period of 1994–2018) [45].



(a)



(b)



(c)

Figure 2. Climatic station installed at the site of Tripoli, Libya, (a) measuring devices (b) pyranometer, type of CMA11 from KIPP & ZONEN. (c) bimetallic actinograph.

2.2. Methodology

The amount of global solar radiation incident at specified surfaces is required for solar photovoltaic designers. In several sites around the world, the average daily horizontal global irradiation is accessible and available; however, the data of solar radiation falling on inclined surfaces are not available [23]. For this reason, a mathematical method to estimate the solar radiation on the inclined surfaces is needed. In this study, the most famous method in this field, known as the Liu and Jordan model, is used to estimate the amount of solar radiation on tilted surfaces.

2.2.1. Extraterrestrial Solar Radiation

The clearness index (k_T) is an important parameter which reflects the ratio of mean daily horizontal global solar radiation (H) to the mean daily extraterrestrial solar radiation (H_0), given by [6]:

$$k_T = H/H_0 \quad (1)$$

The mean daily extraterrestrial solar radiation is defined by [46]:

$$H_0 = \frac{24 I_{sc}}{\pi} \left(1 + 0.033 \cos \frac{360n}{365} \right) \times \left(\cos \varphi \cos \delta \sin \omega_s + \frac{2\pi \omega_s}{360} \sin \varphi \sin \delta \right) \quad (2)$$

where I_{sc} is the value of solar constant (1367 W/m^2), n is the recommended number of the day of the year, tabled in Table 2. δ is the angle of solar declination (degrees), φ is the latitude of the location (degrees), ω_s is the angle of sunrise hour [10,47].

$$\delta = 23.45 \sin \left(360 \frac{284 + n}{365} \right) \quad (3)$$

$$\omega_s = \cos^{-1}(-\tan \varphi \tan \delta) \quad (4)$$

Table 2. Recommended monthly values of the day of the year and declination angles [48].

| Month | Declination | Date | <i>i</i> th Day of the Month | Day of the Year |
|-------|-------------|--------|------------------------------|-----------------|
| Jan | −20.92 | 17 Jan | <i>i</i> | 17 |
| Feb | −12.95 | 16 Feb | 31 + <i>i</i> | 47 |
| Mar | −2.42 | 16 Mar | 59 + <i>i</i> | 75 |
| Apr | 9.41 | 15 Apr | 90 + <i>i</i> | 105 |
| May | 18.79 | 15 May | 120 + <i>i</i> | 135 |
| Jun | 23.09 | 11 Jun | 151 + <i>i</i> | 162 |
| Jul | 21.18 | 17 Jul | 181 + <i>i</i> | 198 |
| Aug | 13.45 | 16 Aug | 212 + <i>i</i> | 228 |
| Sep | 2.22 | 15 Sep | 243 + <i>i</i> | 258 |
| Oct | −9.60 | 15 Oct | 273 + <i>i</i> | 288 |
| Nov | −18.91 | 14 Nov | 304 + <i>i</i> | 318 |
| Dec | −23.05 | 10 Dec | 334 + <i>i</i> | 344 |

2.2.2. Solar Radiation on Tilted Surfaces

The amount of total solar energy incident at the inclined surfaces differs from energy incident on horizontal. The monthly mean daily solar radiation fallen on the inclined surfaces (H_T) is defined by [6]:

$$H_T = RH \quad (5)$$

where R is the value of ratio of the total inclined solar radiation to the horizontal solar radiation. It can be determined based on many components of solar radiation such as beam, diffused and reflected radiation on the inclined surfaces. It is expressed by Liu and Jordan as follows [6]:

$$R = \left(1 - \frac{H_d}{H} \right) R_b + H_d \left(\frac{1 + \cos \beta}{2H} \right) + \rho \left(\frac{1 - \cos \beta}{2} \right) \quad (6)$$

where ρ is ground reflectance, it is selected to be 0.2 in this study [4,6]. β is the tilt angle of the surface of solar photovoltaic module from horizontal. H_d is the monthly average daily diffused solar radiation given by [6]:

$$H_d = H(1.00 - 1.13k_T) \quad (7)$$

R_b is the ratio of the daily direct (beam) solar irradiation on a tilted surface to the daily global solar radiation on a horizontal surface, given as [6,49,50]:

$$R_b = \frac{\cos(\varphi - \beta) \cos \delta \sin \omega'_s + \omega'_s (\pi/180) \sin(\varphi - \beta) \sin \delta}{\cos \varphi \cos \delta \sin \omega_s + \omega_s (\pi/180) \sin \varphi \sin \delta} \quad (8)$$

where ω'_s is the sunset hour angle of the inclined surface given by [6]:

$$\omega'_s = \min \left\{ \begin{array}{l} \omega_s \\ \cos^{-1}(-\tan(\varphi - \beta)\tan\delta) \end{array} \right\} \quad (9)$$

2.2.3. Optimum Tilt Angle

The south-facing optimum tilt angles and the corresponding incident solar radiation were estimated using Liu & Jordan model. The monthly optimum tilt angles of solar PV panel surface for all the studied sites were estimated in such a way that the corresponding total available daily solar radiation is exploited to its maximum level. The tilt angle was changed from 0° to 90° (horizontal to vertical orientation) with 1° resolution. Thus, the optimum tilt angle is the angle corresponding to the maximum solar radiation falling on the tilted surface H_T .

2.2.4. Percentage Gain and Loss in Radiation

The percentage gain in the availability of total solar radiation incidents on inclined surfaces is estimated in the sites under investigation using the following formula [3,5]:

$$\text{Percent Gain (\%)} = \left(\frac{\overline{H}_T|_{\beta=\beta_{opt_i}}}{\overline{H}_T|_{\beta=0}} - 1 \right) \times 100 \quad (10)$$

where i indicates monthly, seasonal, and yearly. And \overline{H}_T is the average of total solar radiation at the specified tilt angle. The reduction in solar radiation due to the annual fixed tilt angle compared to solar radiation available at a monthly optimum tilt angle can be estimated by [3,5]:

$$\text{Percent Loss (\%)} = \left(1 - \frac{\overline{H}_T|_{\beta=\beta_{opt_j}}}{\overline{H}_T|_{\beta_{opt}(\text{monthly})}} - 1 \right) \times 100 \quad (11)$$

where j indicates the seasonal and annual.

2.2.5. Models for Optimum Tilt Angles

The most famous seven empirical models used to determine the optimal tilt angle are shown below [2,6,51]:

- Model #1: linear model

$$\beta_{fit} = a_1\delta + a_0 \quad (12)$$

- Model #2: 2nd-degree polynomial

$$\beta_{fit} = a_2\delta^2 + a_1\delta + a_0 \quad (13)$$

- Model #3: 3rd-degree polynomial

$$\beta_{fit} = a_3\delta^3 + a_2\delta^2 + a_1\delta + a_0 \quad (14)$$

- Model #4: Exponential

$$\beta_{fit} = a_0e^{a_1\delta} \quad (15)$$

- Model #5: Gauss

$$\beta_{fit} = a_0e^{-\left(\frac{\delta-a_1}{a_2}\right)^2} \quad (16)$$

- Model #6: Fourier

$$\beta_{fit} = a_0 + a_1\cos(w\delta) + a_2\sin(w\delta) \quad (17)$$

- Model #7: Exponential II

$$\beta_{fit} = a_0 \left(1 + e^{a_1 \delta}\right) \quad (18)$$

where a_0 , a_1 , a_2 , a_3 , w are regression coefficients.

2.3. Statistical Methods

In this section, different statistical error tests are used to evaluate the established empirical models performance to find out which of them are the most accurate in determining the monthly optimal tilt angles in Libya. These criteria are root mean square error, RMSE, mean bias error, MBE, and correlation coefficient R^2 . They are briefly described below [6,52–54]:

$$RMSE = \sqrt{\frac{1}{k} \sum_{i=1}^k (\beta'_i - \beta_i)^2} \quad (19)$$

$$MBE = \frac{1}{k} \sum_{i=1}^k (\beta'_i - \beta_i) \quad (20)$$

$$R^2 = \frac{1}{k} \sum_{i=1}^k \frac{(\beta_i - \bar{\beta})(\beta'_i - \bar{\beta}')}{\sigma_{\beta} \sigma_{\beta'}} \quad (21)$$

where β'_i and β_i , are the i th estimated and measured optimal tilt angles, respectively. $\bar{\beta}'$ and $\bar{\beta}$ denote the average values of estimated and measured optimal tilt angles. $\sigma_{\beta'}$ and σ_{β} , are the standard deviation of the estimated and measured optimal tilt angles. k is the sample size. The model's performance is also evaluated by the Taylor diagram [55]. It indicates how well the model and experimental data correspond. Three statistical criteria (central root mean square error, correlation coefficient, and standard deviation) are shown by the Taylor diagram in a single two-dimensional graph.

3. Results and Discussion

This case study is performed for twelve major cities in Libya. The aforementioned method is used to determine the optimum tilt angle and its corresponding amount of incident solar radiation for each site. Figure A1 (Appendix B) illustrates the availabilities of monthly average daily solar radiation (in kWh/m²/day) versus different tilt angles for the sites under consideration as mentioned in each figure. Thus, the angle corresponding to the maximum solar radiation falling on the tilted surface is the optimum tilt. For each city, the total tilted solar radiations were plotted versus the tilt angles in two separate figures, from Jan to Jun, and the remaining months of Jul to Dec. The values of monthly optimum tilt angles which correspond to the maximum exploited solar radiation are shown in Table 3. The seasonal optimum tilt angles for the cities under consideration used in winter (Dec, Jan, Feb), spring (Mar, Apr, May), summer (Jun, Jul, Aug), and autumn (Sep, Oct, Nov) are calculated by averaging the corresponding monthly optimum tilt angles. The yearly optimum tilt angle for each city which is fixed throughout the year is also calculated by averaging all monthly optimum tilt angles. The seasonal and annual optimum tilt angles are also presented in Table 3. Figure 3 shows the variation of monthly optimum tilt angle for the selected sites in Libya. As can be seen from the figure, the monthly optimum tilt angle increased during winter and decreased during summer, where it varies from 0° (June and Jul) to 59° (Dec) throughout the year. The results obtained using the model proposed in this study are compared with the modelling method of [37] as shown in Figure 4. Reference [37] used satellite data provided by SolarGIS database to determine the optimum tilt angle in the same region studied in this paper. While the data used in this study are measured at sites, the results are in agreement with reference [37].

Table 3. Optimum monthly, seasonal, and annual tilt angles for the studied sites.

| | | Optimum Tilt Angle β_{Opt} (Degree) | | | | | | | | | | | | |
|--------|-----|-------------------------------------------|----------|------|-------|-------|-----|-----------|---------|-------|----------|------|------|----|
| | | Bengazi | Ajdabiya | Jalu | Kufra | Sebha | Hun | Elgariyat | Tripoli | Nalut | Ghadames | Ghat | Sirt | |
| Months | Jan | 54 | 53 | 54 | 51 | 54 | 53 | 55 | 56 | 54 | 56 | 51 | 53 | |
| | Feb | 46 | 45 | 44 | 41 | 43 | 45 | 45 | 45 | 46 | 47 | 42 | 44 | |
| | Mar | 32 | 31 | 30 | 26 | 29 | 30 | 31 | 34 | 31 | 32 | 26 | 30 | |
| | Apr | 15 | 14 | 13 | 9 | 11 | 13 | 14 | 16 | 14 | 14 | 9 | 14 | |
| | May | 0 | 0 | 0 | 0 | 0 | 0 | 0 | 1 | 0 | 0 | 0 | 0 | |
| | Jun | 0 | 0 | 0 | 0 | 0 | 0 | 0 | 0 | 0 | 0 | 0 | 0 | |
| | Jul | 0 | 0 | 0 | 0 | 0 | 0 | 0 | 0 | 0 | 0 | 0 | 0 | |
| | Aug | 9 | 8 | 7 | 2 | 5 | 7 | 8 | 10 | 9 | 8 | 3 | 8 | |
| | Sep | 26 | 25 | 23 | 19 | 23 | 24 | 23 | 27 | 25 | 25 | 20 | 25 | |
| | Oct | 42 | 40 | 40 | 37 | 40 | 41 | 39 | 43 | 38 | 43 | 38 | 39 | |
| | Nov | 53 | 53 | 51 | 48 | 52 | 52 | 52 | 54 | 50 | 54 | 47 | 51 | |
| | Dec | 56 | 56 | 57 | 52 | 56 | 56 | 57 | 59 | 57 | 57 | 52 | 57 | |
| Season | Jan | Winter | 52 | 51 | 52 | 48 | 51 | 51 | 52 | 53 | 52 | 53 | 48 | 51 |
| | Feb | | 52 | 51 | 52 | 48 | 51 | 51 | 52 | 53 | 52 | 53 | 48 | 51 |
| | Mar | Spring | 16 | 15 | 14 | 12 | 13 | 14 | 15 | 17 | 15 | 15 | 12 | 15 |
| | Apr | | 16 | 15 | 14 | 12 | 13 | 14 | 15 | 17 | 15 | 15 | 12 | 15 |
| | May | | 16 | 15 | 14 | 12 | 13 | 14 | 15 | 17 | 15 | 15 | 12 | 15 |
| | Jun | Summer | 3 | 3 | 2 | 1 | 2 | 2 | 3 | 3 | 3 | 3 | 1 | 3 |
| | Jul | | 3 | 3 | 2 | 1 | 2 | 2 | 3 | 3 | 3 | 3 | 1 | 3 |
| | Aug | | 3 | 3 | 2 | 1 | 2 | 2 | 3 | 3 | 3 | 3 | 1 | 3 |
| | Sep | Autumn | 40 | 39 | 38 | 35 | 38 | 39 | 38 | 41 | 38 | 41 | 35 | 38 |
| | Oct | | 40 | 39 | 38 | 35 | 38 | 39 | 38 | 41 | 38 | 41 | 35 | 38 |
| | Nov | | 40 | 39 | 38 | 35 | 38 | 39 | 38 | 41 | 38 | 41 | 35 | 38 |
| | Dec | | 52 | 51 | 52 | 48 | 51 | 51 | 52 | 53 | 52 | 53 | 48 | 51 |
| Yearly | | 28 | 27 | 27 | 24 | 26 | 27 | 27 | 29 | 27 | 28 | 24 | 27 | |

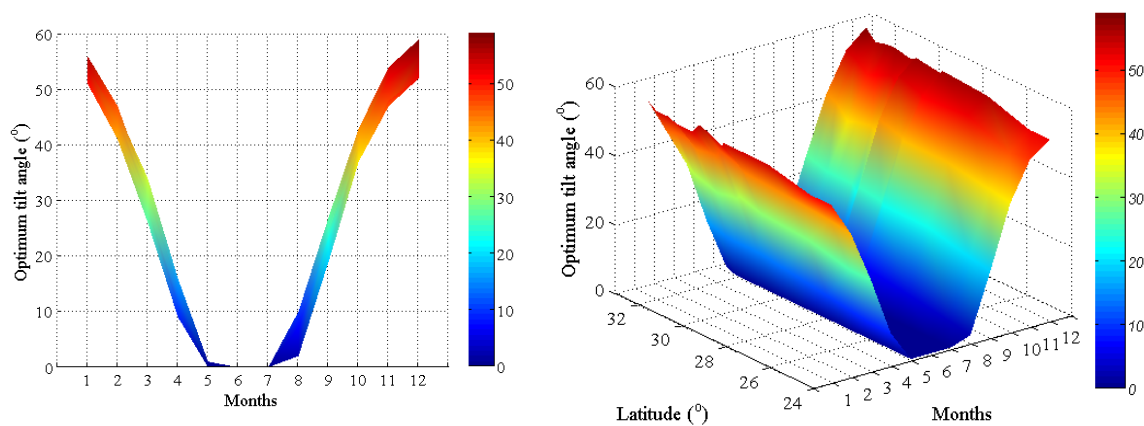


Figure 3. Variation of monthly optimum tilt angle throughout the year.

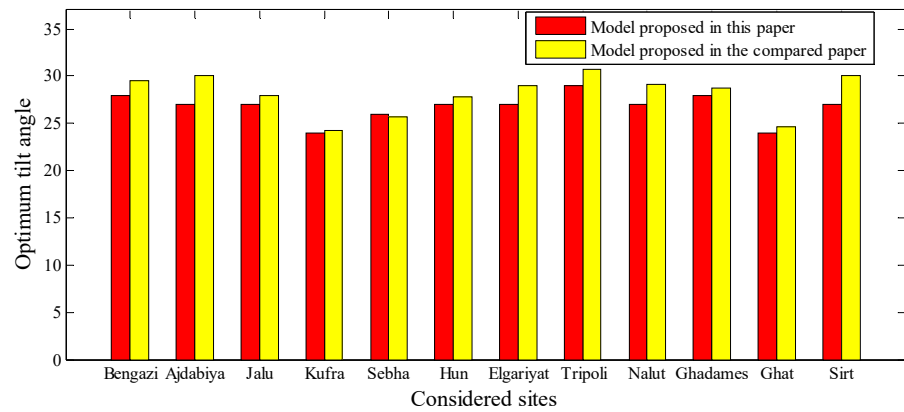


Figure 4. Yearly optimum tilt angle obtained using the model proposed in this paper and in [37].

Total incident solar radiation at different tilted surfaces was estimated and presented in Table A1 (Appendix A). The values of measured horizontal global solar radiation ($\beta = 0$) are presented versus other values of total incident solar at an annual, seasonal, and monthly optimum tilt angle. The values of monthly solar radiation during the period of June to August were the maxima compared to other months. Figure 5 shows the monthly average daily global solar radiation according to tilt angles when the surfaces of PV panels are tilted at the optimum monthly angle, seasonal angle, and yearly angle. From Table A1, the difference in total solar radiation available at yearly, seasonal, and monthly optimum tilt angles is negligible. However, there is a loss (reduction) in solar radiation, because the surfaces are fixed on seasonal or yearly optimum tilt angle compared to solar radiation available at a monthly optimum tilt angle.

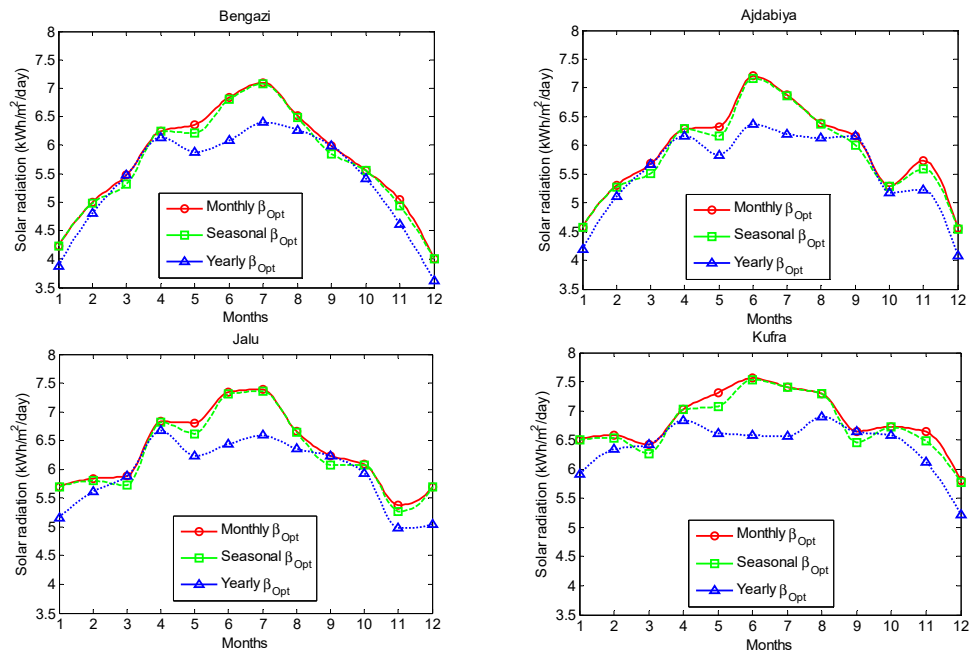


Figure 5. Cont.

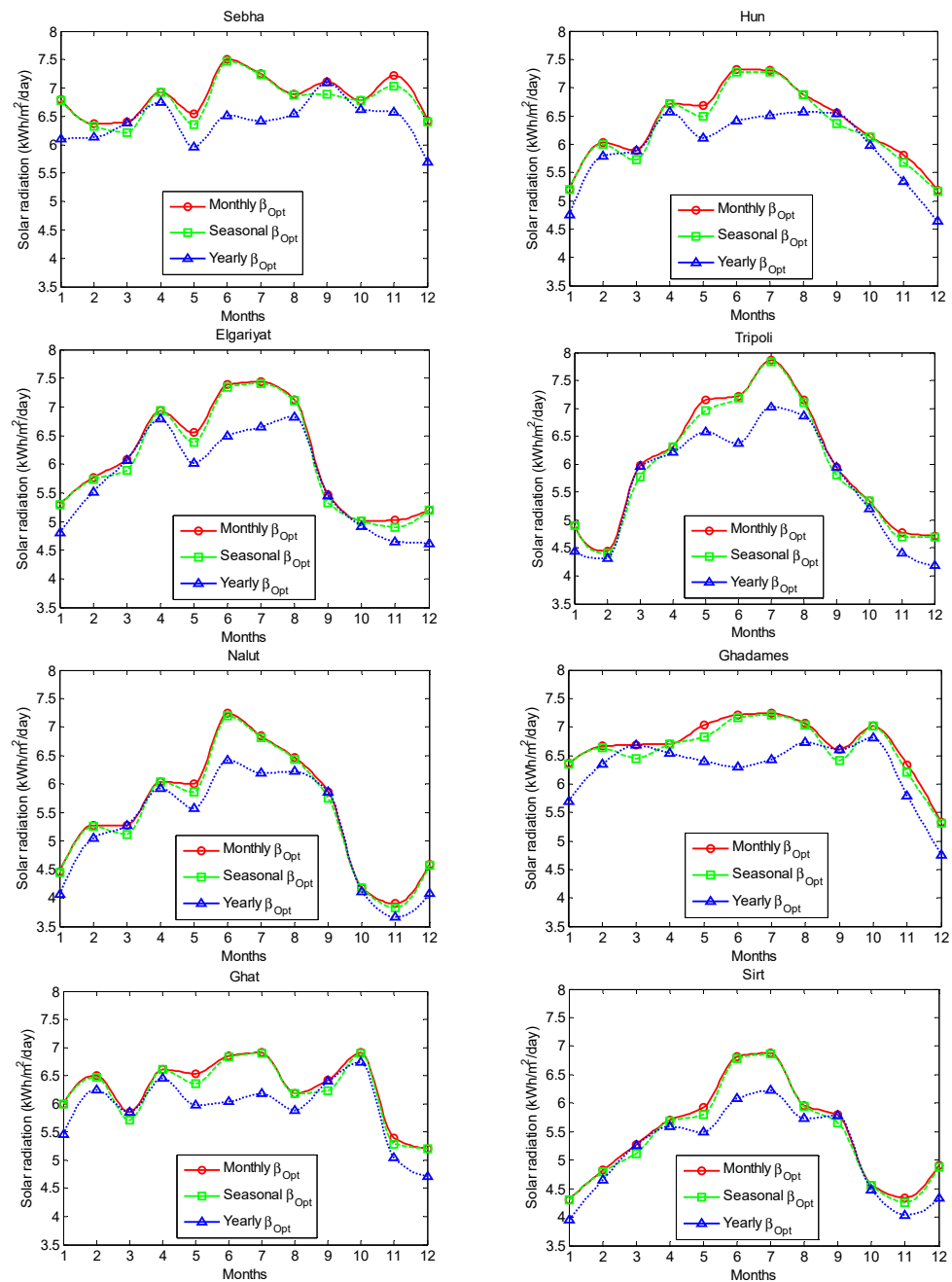


Figure 5. Monthly average daily solar radiation received at different tilt angles.

The percentage increase in the amount of solar radiation falling on the solar PV panel surface obtained for monthly and seasonal optimum tilt angle compared to annual fixed tilt angle is estimated and presented in Table 4.

3.1. Bengazi

Bengazi is located on the northeastern coast of Libya. The monthly average daily total solar radiation varies from 2.57 kWh/m²/day in December up to 7.10 kWh/m²/day in July, with an annual average of 5.01 kWh/m²/day. The monthly optimum tilt angle varies from 0° (in May–July) up to 56° (in December), and the annual optimum tilt angle is 28°. For Bengazi, the percent gain in yearly average total solar radiation incident on the tilted surface ($\bar{H}_T|_{\beta=\beta_{opt_i}}$) in comparison to a horizontal surface is 13.76% at the monthly optimum tilt angle, 12.59% at the seasonal optimum tilt angle, and 7.41% at the annual optimum tilt angle. Energy losses of 1.02% and 5.57% (kWh/m²/day) are determined when the surface

is fixed on seasonal and annual optimum tilt angles, respectively, compared to a surface set on the monthly optimum tilt angle.

Table 4. Percentage gain in radiation falling on monthly and seasonal tilt angle compared to incident radiation at annual fixed tilt angle.

| City | Gain in Monthly Compared to Fixed (%) | Gain in Seasonal Compared to Fixed (%) |
|-----------|---------------------------------------|----------------------------------------|
| Bengazi | 5.95 | 4.83 |
| Ajdabiya | 6.15 | 4.88 |
| Jalu | 6.58 | 5.56 |
| Kufra | 6.89 | 5.79 |
| Sebha | 7.03 | 5.94 |
| Hun | 6.41 | 5.23 |
| Elgariyat | 6.45 | 5.23 |
| Tripoli | 6.39 | 5.15 |
| Nalut | 5.96 | 5.00 |
| Ghadames | 6.87 | 5.59 |
| Ghat | 6.08 | 5.24 |
| Sirt | 6.04 | 5.07 |

3.2. Ajdabiya

Ajdabiya is located in the northeast of Libya. Its yearly average solar radiation falling at the annual optimum tilt angle is 5.01 kWh/m²/day. The monthly optimum tilt angle varies between 0° (in May–July) and 56° (in December), and the annual optimum tilt angle is 27°. The average of total solar radiation falling on different tilt angles is presented in Table A1. The months of June, July, and August had the greatest values of monthly total solar radiation with a peak of 7.21 kWh/m²/day (in July). Whereas the lowest values were recorded during the winter season with a minimum of 2.89 kWh/m²/day (in December). The percent gains in solar radiation incident at monthly, seasonal, and annual optimum tilt angles are 14.04%, 12.82%, and 7.40% more than the horizontal surface ($\beta = 0$). Losses of 1.07% and 5.82% in solar energy are determined with surfaces tilted at seasonal and annual optimum tilt angles, respectively, compared to the surface at monthly optimum tilt angle.

3.3. Jalu

Jalu is located in the east of Libya. The monthly optimum tilt angle varies from 0° in the months of May, June, and July up to 57° in December, and the annual optimum tilt angle is 27°. The monthly averaged daily total solar radiation received at the optimum tilt angle varies from 5.38 kWh/m²/day in November to 7.39 kWh/m²/day in July. The percent gain in total solar radiation falling on PV panel surface at monthly, seasonal, and annual optimum tilt angles is 14.50%, 13.33%, and 7.37% more in comparison to the horizontal surface. The reduction in available solar energy obtained at surfaces inclined to seasonal and annual optimum tilt angles were estimated with percent losses of 1.03% and 6.23%, respectively, compared to surfaces inclined to monthly optimum tilt angle.

3.4. Kufra

Kufra is located in the southeast of Libya. Its monthly total solar radiation incident at optimum tilt angle varies between 5.80 kWh/m²/day in December and 7.56 kWh/m²/day in June with an average annual value of 6.38 kWh/m²/day. The annual optimum tilt angle is 24°, and the monthly optimum tilt angle varies between 0° (in May–July) and 52° in December. Setting the tilt angle of solar PV panels to its monthly and seasonal optimum tilt angles increases the average solar energy with gains of 12.59% and 11.43%, respectively, over that of the horizontal surface. Whereas, tilting the PV panel surface by optimum annual tilt angle which is fixed through the year increases the solar radiation with a gain just of 5.44% more than the horizontal surface. The percent losses in solar radiation incident

at seasonal and annual optimum tilt angles are 1.03% and 6.35%, respectively, less than the surface at the monthly optimum tilt angle.

3.5. Sebha

Sebha is located in the south of Libya. Its yearly average solar radiation falling at the annual optimum tilt angle is 6.85 kWh/m²/day. The average monthly total solar radiation incident on different tilt angles is presented in Table A1. The months of June–August had the greatest values of monthly total solar radiation with a peak of 7.51 kWh/m²/day (in June), and the lowest values were recorded during the winter season with a minimum of 6.42 kWh/m²/day (in December). The monthly optimum tilt angle varies between 0° (in May–July) and 56° (in December), and the annual optimum tilt angle is 26°. The percent gains in the amount of total solar radiation received on PV panels mounted at monthly and seasonal optimum tilt angles with respect to horizontal surface are 16.02% and 14.72% respectively, and the average of 8.37% percent gain in total solar radiation obtained at annual optimum tilt angle more than horizontal surface. The surfaces of PV panels mounted at seasonal and annual optimum tilt angles were determined to have losses of 1.12% and 6.60%, respectively, compared to surfaces changed according to monthly optimum tilt angle.

3.6. Hun

Hun is located in the center of Libya. The monthly average daily total solar radiation received at the monthly optimum tilt angle varies from 5.19 kWh/m²/day in December up to 7.32 kWh/m²/day in June, with an annual average of 6.31 kWh/m²/day. The monthly optimum tilt angle varies from 0° (in May–July) up to 56° (in December), and the annual optimum tilt angle is 27°. For Hun, the percent gain in yearly average total solar radiation incident on the tilted surface ($\bar{H}_T|_{\beta=\beta_{opt}}$) in comparison to a horizontal surface is 14.22% at the monthly optimum tilt angle, 13.03% at the seasonal optimum tilt angle, and 7.28% at the annual optimum tilt angle. Energy losses of 1.04% and 6.08% (kWh/m²/day) are determined when the surface is fixed on seasonal and annual optimum tilt angles, respectively, compared to a surface set on the monthly optimum tilt angle.

3.7. Elgariyat

The yearly average solar radiation falling at the annual optimum tilt angle is 6.11 kWh/m²/day. The average of total solar radiation falling on different tilt angles is presented in Table A1. The months of June, July, and August had the greatest values of monthly total solar radiation with a peak of 7.44 kWh/m²/day (in July). The monthly optimum tilt angle varies between 0° (in May–July) and 57° (in December), and the annual optimum tilt angle is 27°. The percent gains in solar radiation incident at monthly, seasonal, and annual optimum tilt angles are 13.97%, 12.77%, and 7.04% more than the horizontal surface ($\beta = 0$). Losses of 1.05% and 6.08% in solar energy are determined with surfaces tilted at seasonal and annual optimum tilt angles, respectively, compared to surfaces at monthly optimum tilt angle.

3.8. Tripoli

Tripoli is the capital of Libya, and it is a coastal city located in the north. The monthly optimum tilt angle varies from 0° in the months of June, and July up to 59° in December, and the annual optimum tilt angle is 29°. The monthly averaged daily total solar radiation received at the optimum tilt angle varies from 4.72 kWh/m²/day in November to 7.87 kWh/m²/day in July. The percent gains in total solar radiation falling on the PV panels surfaces at monthly, seasonal, and annual optimum tilt angles are 14.46%, 13.17%, and 7.60% more in comparison to the horizontal surface. The reduction in available solar energy obtained at surfaces inclined to seasonal and annual optimum tilt angles was estimated with percent losses of 1.13% and 6.00%, respectively, compared to surfaces inclined to monthly optimum tilt angle.

3.9. Nalut

Nalut is located in the northwest of Libya. Its monthly total solar radiation incident at optimum tilt angle varies between 4.46 kWh/m²/day in January and 7.24 kWh/m²/day in June with an average annual value of 5.51 kWh/m²/day. The annual optimum tilt angle is 27°, and the monthly optimum tilt angle varies between 0° (in May–July) and 57° in December. Setting the tilt angle of solar PV panels to its monthly and seasonal optimum tilt angles increases the average solar energy with gains of 12.69% and 11.68%, respectively, over that of the horizontal surface. Whereas, tilting the PV panel surface by optimum annual tilt angle which is fixed through the year increases the solar radiation with a gain just of 6.42% more than the horizontal surface. The percent losses in solar radiation incident at seasonal and annual optimum tilt angles are 0.90% and 5.57%, respectively, less than the surfaces at the monthly optimum tilt angle.

3.10. Ghadames

Ghadames is located in the west of Libya. Its yearly average solar radiation falling at the annual optimum tilt angle is 6.69 kWh/m²/day. The average monthly total solar radiation incident on different tilt angles is presented in Table A1. The months of June–August had the greatest values of monthly total solar radiation with a peak of 7.24 kWh/m²/day (in July), and the lowest values were recorded during the winter season with a minimum of 5.32 kWh/m²/day (in December). The monthly optimum tilt angle varies between 0° (in May–July) and 57° (in December), and the annual optimum tilt angle is 28°. The percent gains in the amount of total solar radiation received on PV panels mounted at monthly and seasonal optimum tilt angles with respect to horizontal surface are 17.24% and 15.87% respectively, and the average of 9.71% percent gain in total solar radiation obtained at annual optimum tilt angle more than horizontal surface. The surfaces of PV panels mounted at seasonal and annual optimum tilt angles were determined to have losses of 1.17% and 6.42%, respectively, compared to surfaces changed according to monthly optimum tilt angle.

3.11. Ghat

Ghat is located in the southwest of Libya. The monthly average daily total solar radiation received at the monthly optimum tilt angle varies from 5.21 kWh/m²/day in December up to 6.91 kWh/m²/day in July, with an annual average of 6.28 kWh/m²/day. The monthly optimum tilt angle varies from 0° (in May–July) up to 52° (in December), and the annual optimum tilt angle is 24°. For Ghat, the percent gain in yearly average total solar radiation incident on the tilted surface ($\overline{H}_T|_{\beta=\beta_{opt}}$) in comparison to a horizontal surface is 12.43% at the monthly optimum tilt angle, 11.41% at the seasonal optimum tilt angle, and 5.87% at the annual optimum tilt angle. Energy losses of 0.91% and 5.83% (kWh/m²/day) are determined when the surface is fixed on seasonal and annual optimum tilt angles, respectively, compared to a surface set on the monthly optimum tilt angle.

3.12. Sirt

Sirt is a coastal city located in the north of Libya. The monthly optimum tilt angle varies from 0° in the months of May, June, and July up to 57° in December, and the annual optimum tilt angle is 27°. The monthly average daily total solar radiation received at the optimum tilt angle varies from 4.91 kWh/m²/day in November to 6.88 kWh/m²/day in July. The percent gains in total solar radiation falling on the PV panel surface at monthly, seasonal, and annual optimum tilt angles are 13.00%, 11.93%, and 6.67% more in comparison to the horizontal surface. Percent losses of 0.95% and 5.60% in solar radiation incident on the surface of PV panels mounted at the seasonal and annual optimum tilt angles, respectively, were observed compared to the monthly optimum tilt angle.

The measured data of global solar radiation were used to estimate the monthly optimum tilt angles for all studied sites in Libya, thus they were employed for establishing the presented seven empirical models to predict the optimal tilt angle as shown in Figure 6.

The Levenberg–Marquardt method (non-linear regression) provided by MATLAB toolbox is used to determine the empirical coefficients of the empirical models. They are shown in Table 5. To find out which of the presented models are the most accurate in determining the monthly optimal tilt angles, their performances are assessed using the aforementioned statistical criteria. The results are shown in Table 5. The Taylor diagram shown in Figure 7 is used to rank the model’s performance. The model which has a point in the diagram located at the down and left is the best. The best models are illustrated in bold in Table 5. As can be clearly seen from the Table 5 and Figure 7, both 3rd-order polynomial model and Fourier model have the highest value of *R*, thus they can be considered the best models for determining the optimal tilt angle in Libya, given as:

$$\beta_{fit} = 0.0005262\delta^3 + 0.001501\delta^2 - 1.519\delta + 26.51 \tag{22}$$

$$\beta_{fit} = 27.95 - 1.421\cos(0.04696\delta) - 32.39\sin(0.04696\delta) \tag{23}$$

whereas both exponential models were found to be inefficient in determining the optimum tilt angle.

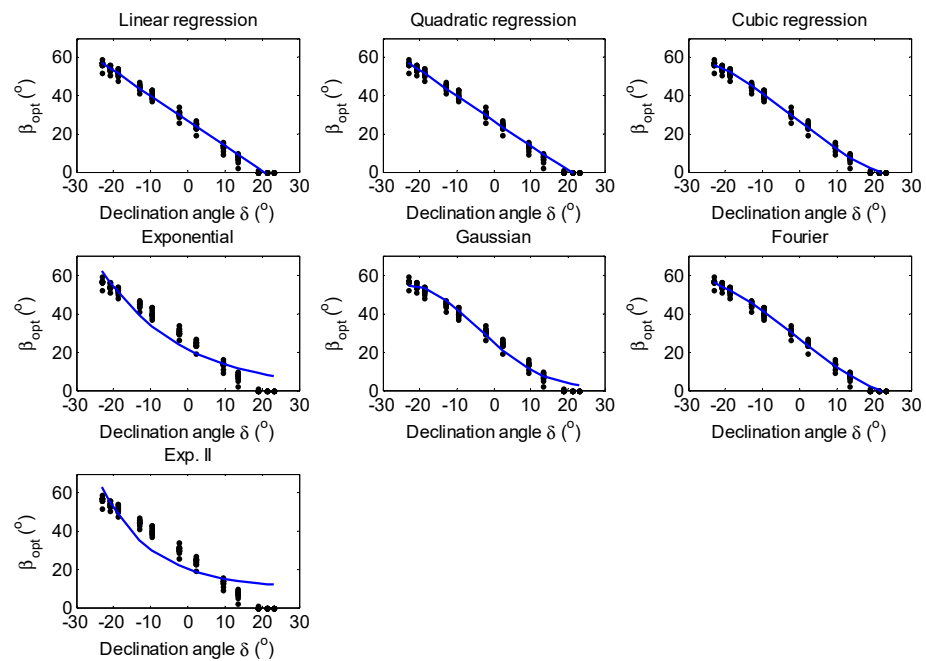


Figure 6. Fitting empirical models to the measured optimum tilt angles of solar PV panels in Libya.

Table 5. Regression coefficients of the empirical models and their statistical criteria. The best models are illustrated in bold.

| Model No. | Regression Coefficients | | | | Statistical Criteria | | | |
|-----------|-------------------------|-----------------------|-----------------------|-----------------------|----------------------|----------------|---------------|---------------|
| | <i>a</i> ₀ | <i>a</i> ₁ | <i>a</i> ₂ | <i>a</i> ₃ | <i>W</i> | MBE | RMSE | <i>R</i> |
| 1 | 26.93 | −1.307 | | | | −0.0017 | 2.0895 | 0.9883 |
| 2 | 26.53 | −1.307 | 0.001511 | | | −0.0049 | 2.0696 | 0.9884 |
| 3 | 26.51 | −1.519 | 0.001501 | 0.0005262 | | 0.0015 | 1.7136 | 0.9899 |
| 4 | 21.44 | −0.04614 | | | | −1.0423 | 5.9915 | 0.9573 |
| 5 | 54.59 | −23.38 | 26.27 | | | −0.4846 | 2.6419 | 0.9862 |
| 6 | 27.95 | −1.421 | −32.39 | | 0.04696 | −0.0050 | 1.7203 | 0.9899 |
| 7 | 10.04 | −0.07208 | | | | −1.4062 | 8.5018 | 0.9200 |

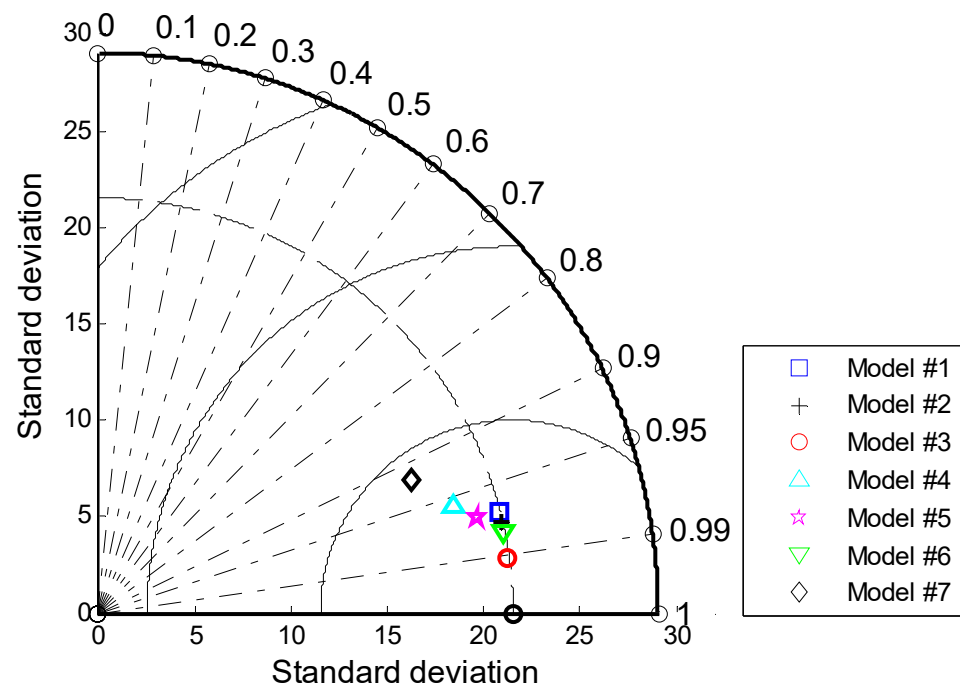


Figure 7. Taylor diagram for the presented models applied on the studied sites in Libya.

4. Conclusions

In this study, monthly, seasonal, and annual optimum tilt angles in twelve major Libyan cities were estimated. Due to the differences in the sun's position throughout the year, the months have different values of optimum tilt angles. The conclusions are as follows:

- The summer season has a value of optimum tilt angle lower than the winter season. The monthly optimum tilt angles in the studied sites vary from 0° (in June and July) to 59° (in December). Also, the annual optimum tilt angles for the selected sites vary between 24° and 29° .
- The percent gain in annual average solar energy ($\text{kWh}/\text{m}^2/\text{day}$) received at the surfaces of PV panels mounted at monthly optimum tilt angle varies from 12.43% to 17.24% for all cities compared to the horizontal surface.
- The percentage increase in solar radiation due to seasonal optimum tilt angle compared with annual fixed tilt angle for all cities varies between 4.83% and 5.94%.
- A loss of 5.57–6.60% in solar energy ($\text{kWh}/\text{m}^2/\text{day}$) is determined with surfaces tilted at the annual optimum tilt angle compared to surfaces at monthly optimum tilt angle.
- Both the third-order polynomial model and the Fourier model had the best performance in estimating the optimum tilt angle in Libya.

From the results presented in the study, it is recommended that the solar surfaces should be tilted according to seasonal or monthly optimum tilt angle for better exploitation of total solar radiation. Although there is solar energy loss in PV systems, when the tilt angle of PV panels is fixed at the annual optimum tilt angle, it can be used when changing the angle of panels is not possible due to the cost of installation.

Author Contributions: A.A.T.: Conceptualization, Methodology, Software, Investigation, Writing original draft, Visualization. F.M.: Conceptualization, Methodology. All authors have read and agreed to the published version of the manuscript.

Funding: The article processing charges (APC) was funded by Federation of Arab Scientific Research Councils (FASRC).

Data Availability Statement: The original contributions presented in the study are included in the article, further inquiries can be directed to the corresponding author.

Conflicts of Interest: The authors declare no conflicts of interest.

Nomenclature

| | |
|-------------------------|----------------------------------------------------------------------------------------------|
| a_0, a_1, a_2, a_3, w | Regression coefficient |
| H | Global solar radiation on a horizontal surface |
| H_0 | Extraterrestrial solar radiation |
| H_d | Diffuse solar radiation |
| H_T | Solar radiation incident on a tilted surface |
| I_{sc} | Solar constant |
| k_T | Clearness index |
| MBE | Mean bias error |
| n | Number of the day of the year |
| R^2 | Correlation coefficient |
| R | Ratio of the tilted solar radiation to the horizontal solar radiation |
| R_b | Ratio of the direct solar radiation on the tilted surface to the horizontal solar radiation. |
| $RMSE$ | Root mean square error. |
| φ | Latitude |
| δ | Solar declination |
| ω_s | Sunrise hour angle |
| ω'_s | Sunset hour angle |
| β | Tilt angle |

Appendix A

Table A1. Total available solar radiation (kWh/m²/day) for south-facing panel surfaces at monthly, seasonal, and annual tilt angles.

| Months | Bengazi | | | | Ajdabiya | | | |
|---------|-----------------------|----------------------------------|----------------------------------|---------------------------------|-----------------------|----------------------------------|----------------------------------|---------------------------------|
| | $\bar{H}_T \beta=0$ | $\bar{H}_T \beta=\text{mont.}$ | $\bar{H}_T \beta=\text{seas.}$ | $\bar{H}_T \beta=\text{ann.}$ | $\bar{H}_T \beta=0$ | $\bar{H}_T \beta=\text{mont.}$ | $\bar{H}_T \beta=\text{seas.}$ | $\bar{H}_T \beta=\text{ann.}$ |
| Jan | 2.82 | 4.23 | 4.23 | 3.88 | 3.07 | 4.58 | 4.58 | 4.19 |
| Feb | 3.80 | 5.00 | 4.98 | 4.81 | 4.06 | 5.31 | 5.28 | 5.11 |
| Mar | 4.84 | 5.48 | 5.31 | 5.47 | 5.05 | 5.68 | 5.51 | 5.67 |
| Apr | 6.09 | 6.25 | 6.25 | 6.14 | 6.15 | 6.29 | 6.29 | 6.17 |
| May | 6.36 | 6.36 | 6.21 | 5.88 | 6.32 | 6.32 | 6.16 | 5.83 |
| Jun | 6.84 | 6.84 | 6.80 | 6.08 | 7.21 | 7.21 | 7.17 | 6.37 |
| Jul | 7.10 | 7.10 | 7.08 | 6.40 | 6.88 | 6.88 | 6.86 | 6.20 |
| Aug | 6.46 | 6.52 | 6.49 | 6.27 | 6.35 | 6.39 | 6.37 | 6.13 |
| Sep | 5.52 | 5.99 | 5.85 | 5.99 | 5.71 | 6.16 | 6.01 | 6.16 |
| Oct | 4.38 | 5.56 | 5.56 | 5.42 | 4.29 | 5.29 | 5.29 | 5.18 |
| Nov | 3.34 | 5.04 | 4.93 | 4.62 | 3.76 | 5.74 | 5.59 | 5.23 |
| Dec | 2.57 | 4.01 | 4.01 | 3.62 | 2.89 | 4.55 | 4.54 | 4.08 |
| Average | 5.01 | 5.70 | 5.64 | 5.38 | 5.15 | 5.87 | 5.80 | 5.53 |
| % Gain | - | 13.76 | 12.59 | 7.41 | - | 14.04 | 12.82 | 7.40 |

Table A1. Cont.

| Months | Jalu | | | | Kufra | | | |
|---------|--------------------------|-------------------------------------|-------------------------------------|------------------------------------|--------------------------|-------------------------------------|-------------------------------------|------------------------------------|
| | $\overline{H}_T \beta=0$ | $\overline{H}_T \beta=\text{mont.}$ | $\overline{H}_T \beta=\text{seas.}$ | $\overline{H}_T \beta=\text{ann.}$ | $\overline{H}_T \beta=0$ | $\overline{H}_T \beta=\text{mont.}$ | $\overline{H}_T \beta=\text{seas.}$ | $\overline{H}_T \beta=\text{ann.}$ |
| Jan | 3.70 | 5.70 | 5.70 | 5.16 | 4.47 | 6.51 | 6.50 | 5.91 |
| Feb | 4.47 | 5.84 | 5.80 | 5.61 | 5.24 | 6.58 | 6.54 | 6.34 |
| Mar | 5.28 | 5.88 | 5.72 | 5.88 | 5.91 | 6.42 | 6.27 | 6.42 |
| Apr | 6.69 | 6.83 | 6.82 | 6.68 | 6.97 | 7.03 | 7.02 | 6.84 |
| May | 6.81 | 6.81 | 6.62 | 6.23 | 7.31 | 7.31 | 7.08 | 6.62 |
| Jun | 7.35 | 7.35 | 7.31 | 6.44 | 7.56 | 7.56 | 7.54 | 6.58 |
| Jul | 7.39 | 7.39 | 7.36 | 6.59 | 7.41 | 7.41 | 7.40 | 6.56 |
| Aug | 6.63 | 6.66 | 6.65 | 6.36 | 7.29 | 7.29 | 7.29 | 6.90 |
| Sep | 5.83 | 6.24 | 6.08 | 6.23 | 6.35 | 6.65 | 6.46 | 6.64 |
| Oct | 4.89 | 6.09 | 6.08 | 5.94 | 5.61 | 6.73 | 6.72 | 6.58 |
| Nov | 3.72 | 5.38 | 5.27 | 4.98 | 4.72 | 6.64 | 6.48 | 6.12 |
| Dec | 3.50 | 5.70 | 5.69 | 5.05 | 3.93 | 5.80 | 5.78 | 5.22 |
| Average | 5.52 | 6.32 | 6.26 | 5.93 | 6.06 | 6.83 | 6.76 | 6.39 |
| % Gain | - | 14.50 | 13.33 | 7.37 | - | 12.59 | 11.43 | 5.44 |
| Months | Sebha | | | | Hun | | | |
| | $\overline{H}_T \beta=0$ | $\overline{H}_T \beta=\text{mont.}$ | $\overline{H}_T \beta=\text{seas.}$ | $\overline{H}_T \beta=\text{ann.}$ | $\overline{H}_T \beta=0$ | $\overline{H}_T \beta=\text{mont.}$ | $\overline{H}_T \beta=\text{seas.}$ | $\overline{H}_T \beta=\text{ann.}$ |
| Jan | 4.35 | 6.79 | 6.78 | 6.11 | 3.47 | 5.20 | 5.20 | 4.75 |
| Feb | 4.92 | 6.37 | 6.33 | 6.13 | 4.58 | 6.03 | 6.00 | 5.79 |
| Mar | 5.77 | 6.40 | 6.22 | 6.39 | 5.28 | 5.89 | 5.72 | 5.88 |
| Apr | 6.83 | 6.93 | 6.93 | 6.75 | 6.59 | 6.72 | 6.72 | 6.57 |
| May | 6.55 | 6.55 | 6.36 | 5.96 | 6.68 | 6.68 | 6.49 | 6.11 |
| Jun | 7.51 | 7.51 | 7.48 | 6.52 | 7.32 | 7.32 | 7.28 | 6.41 |
| Jul | 7.25 | 7.25 | 7.23 | 6.42 | 7.31 | 7.31 | 7.28 | 6.51 |
| Aug | 6.87 | 6.89 | 6.88 | 6.54 | 6.85 | 6.88 | 6.87 | 6.57 |
| Sep | 6.65 | 7.11 | 6.89 | 7.10 | 6.09 | 6.55 | 6.36 | 6.54 |
| Oct | 5.46 | 6.78 | 6.78 | 6.62 | 4.91 | 6.13 | 6.12 | 5.98 |
| Nov | 4.75 | 7.22 | 7.04 | 6.57 | 3.92 | 5.81 | 5.68 | 5.34 |
| Dec | 3.97 | 6.42 | 6.40 | 5.69 | 3.28 | 5.19 | 5.17 | 4.64 |
| Average | 5.91 | 6.85 | 6.78 | 6.40 | 5.52 | 6.31 | 6.24 | 5.93 |
| % Gain | - | 16.02 | 14.72 | 8.37 | - | 14.22 | 13.03 | 7.28 |

Table A1. Cont.

| Months | Elgariyat | | | | Tripoli | | | |
|---------|--------------------------|-------------------------------------|-------------------------------------|------------------------------------|--------------------------|-------------------------------------|-------------------------------------|------------------------------------|
| | $\overline{H}_T \beta=0$ | $\overline{H}_T \beta=\text{mont.}$ | $\overline{H}_T \beta=\text{seas.}$ | $\overline{H}_T \beta=\text{ann.}$ | $\overline{H}_T \beta=0$ | $\overline{H}_T \beta=\text{mont.}$ | $\overline{H}_T \beta=\text{seas.}$ | $\overline{H}_T \beta=\text{ann.}$ |
| Jan | 3.43 | 5.30 | 5.30 | 4.80 | 3.07 | 4.91 | 4.91 | 4.44 |
| Feb | 4.35 | 5.77 | 5.73 | 5.52 | 3.44 | 4.45 | 4.41 | 4.31 |
| Mar | 5.38 | 6.08 | 5.89 | 6.07 | 5.18 | 5.98 | 5.78 | 5.96 |
| Apr | 6.76 | 6.93 | 6.93 | 6.79 | 6.14 | 6.32 | 6.32 | 6.21 |
| May | 6.55 | 6.55 | 6.38 | 6.02 | 7.15 | 7.15 | 6.96 | 6.58 |
| Jun | 7.39 | 7.39 | 7.35 | 6.50 | 7.22 | 7.22 | 7.18 | 6.37 |
| Jul | 7.44 | 7.44 | 7.41 | 6.65 | 7.87 | 7.87 | 7.84 | 7.03 |
| Aug | 7.08 | 7.13 | 7.11 | 6.83 | 7.06 | 7.15 | 7.11 | 6.87 |
| Sep | 5.13 | 5.46 | 5.32 | 5.45 | 5.46 | 5.95 | 5.80 | 5.95 |
| Oct | 4.13 | 5.01 | 5.01 | 4.92 | 4.20 | 5.34 | 5.34 | 5.21 |
| Nov | 3.46 | 5.02 | 4.90 | 4.65 | 3.17 | 4.78 | 4.69 | 4.41 |
| Dec | 3.20 | 5.20 | 5.19 | 4.62 | 2.81 | 4.72 | 4.70 | 4.19 |
| Average | 5.36 | 6.11 | 6.04 | 5.74 | 5.23 | 5.99 | 5.92 | 5.63 |
| % Gain | - | 13.97 | 12.77 | 7.04 | - | 14.46 | 13.17 | 7.60 |
| Months | Nalut | | | | Ghadames | | | |
| | $\overline{H}_T \beta=0$ | $\overline{H}_T \beta=\text{mont.}$ | $\overline{H}_T \beta=\text{seas.}$ | $\overline{H}_T \beta=\text{ann.}$ | $\overline{H}_T \beta=0$ | $\overline{H}_T \beta=\text{mont.}$ | $\overline{H}_T \beta=\text{seas.}$ | $\overline{H}_T \beta=\text{ann.}$ |
| Jan | 2.96 | 4.46 | 4.45 | 4.06 | 3.89 | 6.36 | 6.35 | 5.70 |
| Feb | 3.99 | 5.28 | 5.25 | 5.05 | 4.85 | 6.66 | 6.63 | 6.35 |
| Mar | 4.71 | 5.28 | 5.12 | 5.27 | 5.84 | 6.69 | 6.45 | 6.68 |
| Apr | 5.90 | 6.04 | 6.04 | 5.93 | 6.55 | 6.70 | 6.70 | 6.54 |
| May | 6.00 | 6.00 | 5.86 | 5.57 | 7.03 | 7.03 | 6.82 | 6.40 |
| Jun | 7.24 | 7.24 | 7.20 | 6.42 | 7.21 | 7.21 | 7.17 | 6.30 |
| Jul | 6.84 | 6.84 | 6.82 | 6.19 | 7.24 | 7.24 | 7.21 | 6.43 |
| Aug | 6.41 | 6.46 | 6.44 | 6.22 | 7.01 | 7.06 | 7.04 | 6.73 |
| Sep | 5.43 | 5.86 | 5.75 | 5.86 | 6.10 | 6.60 | 6.41 | 6.60 |
| Oct | 3.51 | 4.17 | 4.17 | 4.11 | 5.38 | 7.02 | 7.02 | 6.81 |
| Nov | 2.82 | 3.90 | 3.83 | 3.66 | 4.08 | 6.34 | 6.20 | 5.79 |
| Dec | 2.85 | 4.59 | 4.57 | 4.08 | 3.26 | 5.32 | 5.31 | 4.76 |
| Average | 4.89 | 5.51 | 5.46 | 5.20 | 5.70 | 6.69 | 6.61 | 6.26 |
| % Gain | - | 12.69 | 11.68 | 6.42 | - | 17.24 | 15.87 | 9.71 |

Table A1. Cont.

| Months | Ghat | | | | Sirt | | | |
|---------|-----------------------------|----------------------------------------|----------------------------------------|---------------------------------------|-----------------------------|----------------------------------------|----------------------------------------|---------------------------------------|
| | $\overline{H}_T _{\beta=0}$ | $\overline{H}_T _{\beta=\text{mont.}}$ | $\overline{H}_T _{\beta=\text{seas.}}$ | $\overline{H}_T _{\beta=\text{ann.}}$ | $\overline{H}_T _{\beta=0}$ | $\overline{H}_T _{\beta=\text{mont.}}$ | $\overline{H}_T _{\beta=\text{seas.}}$ | $\overline{H}_T _{\beta=\text{ann.}}$ |
| Jan | 4.14 | 5.99 | 5.99 | 5.45 | 2.92 | 4.31 | 4.31 | 3.95 |
| Feb | 5.13 | 6.51 | 6.47 | 6.25 | 3.75 | 4.82 | 4.79 | 4.65 |
| Mar | 5.40 | 5.85 | 5.71 | 5.85 | 4.72 | 5.27 | 5.12 | 5.26 |
| Apr | 6.55 | 6.61 | 6.61 | 6.45 | 5.58 | 5.70 | 5.69 | 5.59 |
| May | 6.54 | 6.54 | 6.36 | 5.98 | 5.92 | 5.92 | 5.79 | 5.49 |
| Jun | 6.85 | 6.85 | 6.83 | 6.04 | 6.82 | 6.82 | 6.79 | 6.08 |
| Jul | 6.91 | 6.91 | 6.90 | 6.18 | 6.88 | 6.88 | 6.86 | 6.22 |
| Aug | 6.18 | 6.19 | 6.18 | 5.89 | 5.92 | 5.96 | 5.94 | 5.73 |
| Sep | 6.11 | 6.42 | 6.24 | 6.40 | 5.38 | 5.79 | 5.66 | 5.78 |
| Oct | 5.67 | 6.91 | 6.90 | 6.74 | 3.79 | 4.56 | 4.56 | 4.48 |
| Nov | 3.99 | 5.39 | 5.29 | 5.04 | 3.07 | 4.34 | 4.26 | 4.04 |
| Dec | 3.58 | 5.21 | 5.21 | 4.72 | 3.01 | 4.91 | 4.88 | 4.33 |
| Average | 5.59 | 6.28 | 6.23 | 5.92 | 4.81 | 5.44 | 5.39 | 5.13 |
| % Gain | - | 12.43 | 11.41 | 5.87 | - | 13.00 | 11.93 | 6.67 |

Appendix B

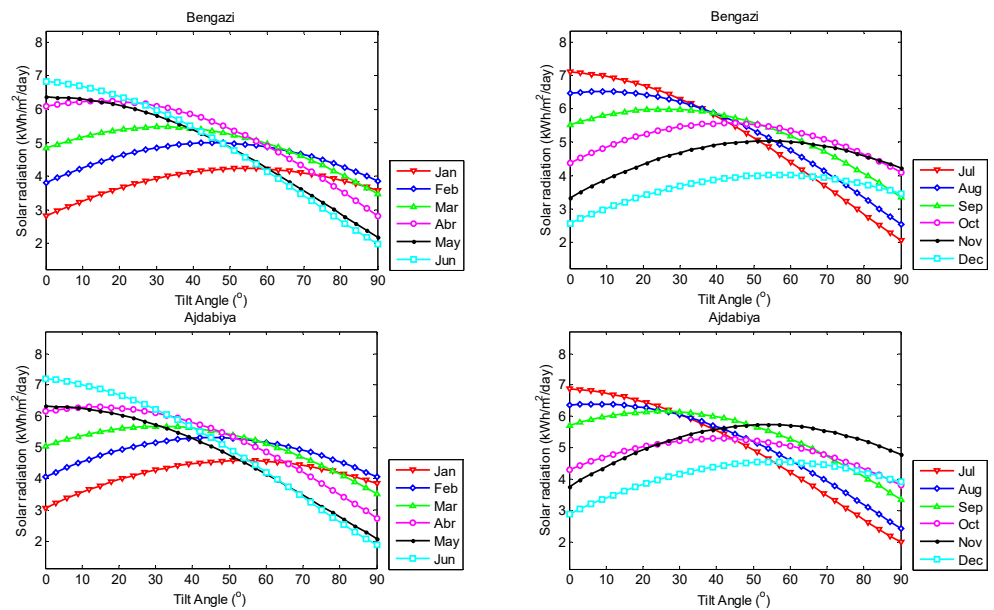


Figure A1. Cont.

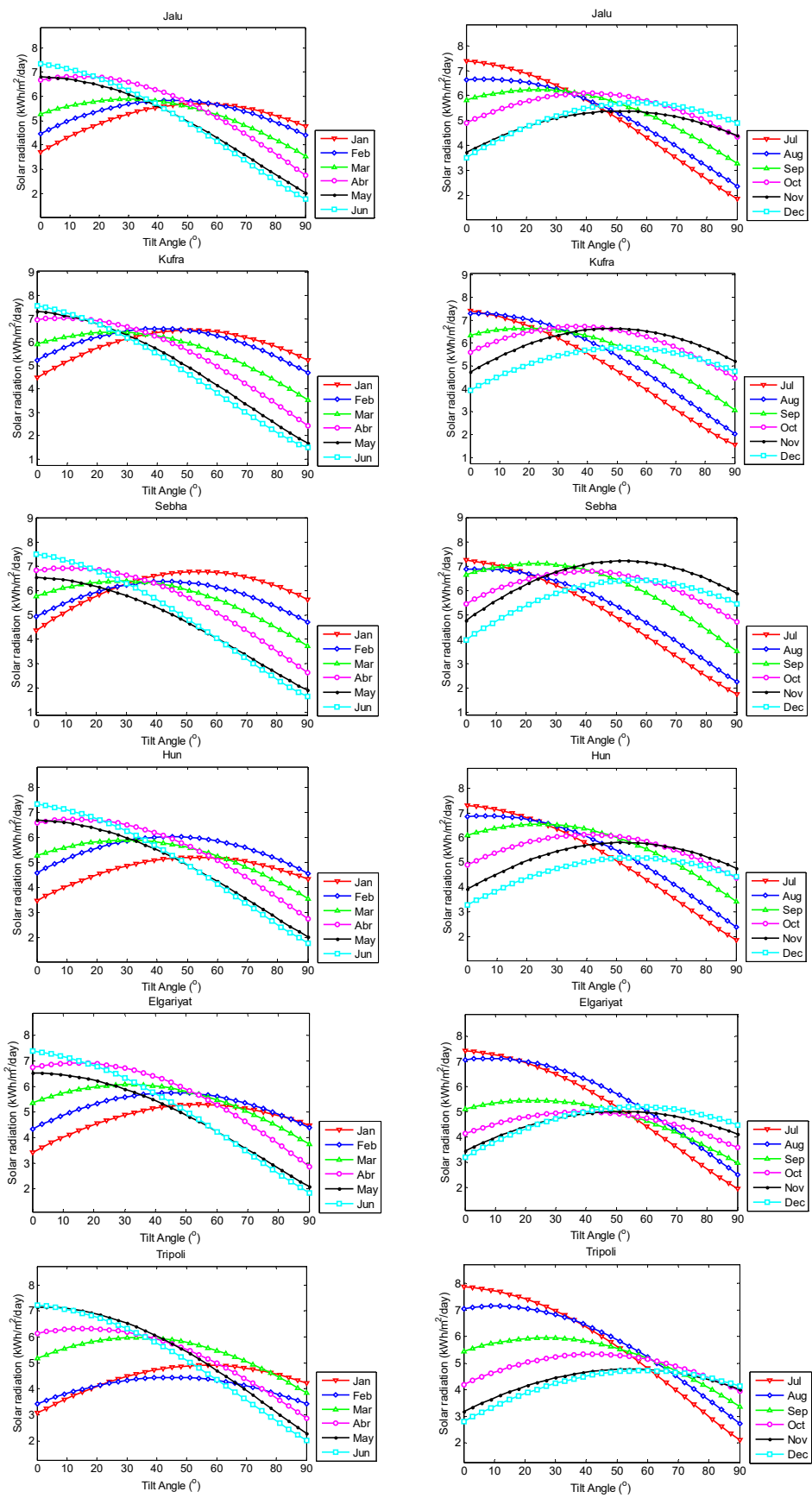


Figure A1. Cont.

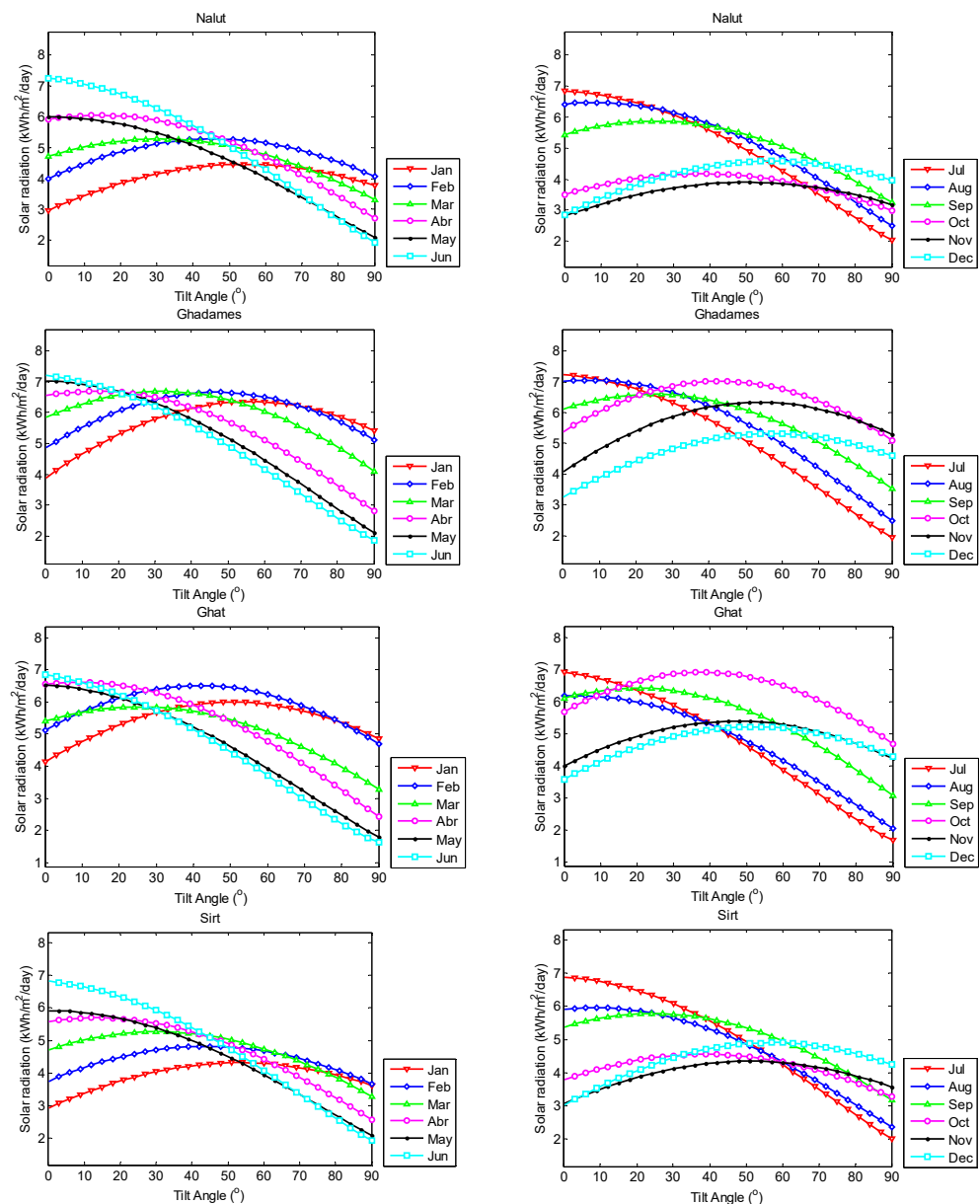


Figure A1. The availability of monthly average daily solar radiation on tilted surfaces, (January–June, and July–December).

References

1. Obiwulu, A.U.; Erusiafe, N.; Olopade, M.A.; Nwokolo, S.C. Modeling and estimation of the optimal tilt angle, maximum incident solar radiation, and global radiation index of the photovoltaic system. *Heliyon* **2022**, *8*, e09598. [[CrossRef](#)] [[PubMed](#)]
2. Hassan, Q.; Abbas, M.K.; Abdulateef, A.M.; Abdulateef, J.; Mohamad, A. Assessment the potential solar energy with the models for optimum tilt angles of maximum solar irradiance for Iraq. *Case Stud. Chem. Environ. Eng.* **2021**, *4*, 100140. [[CrossRef](#)]
3. Jamil, B.; Siddiqui, A.T.; Akhtar, N. Estimation of solar radiation and optimum tilt angles for south-facing surfaces in Humid Subtropical Climatic Region of India. *Eng. Sci. Technol. Int. J.* **2016**, *19*, 1826–1835. [[CrossRef](#)]
4. Mansour, R.B.; Khan, M.A.; Alsulaiman, F.A.; Mansour, R.B. Optimizing the solar PV tilt angle to maximize the power output: A case study for Saudi Arabia. *IEEE Access* **2021**, *9*, 15914–15928. [[CrossRef](#)]
5. Alqaed, S.; Mustafa, J.; Almeahmedi, F.A.; Jamil, B. Estimation of ideal tilt angle for solar-PV panel surfaces facing south: A case study for Najran City, Saudi Arabia. *J. Therm. Anal. Calorim.* **2023**, *148*, 8641–8654. [[CrossRef](#)]
6. Bakirci, K. General models for optimum tilt angles of solar panels: Turkey case study. *Renew. Sustain. Energy Rev.* **2012**, *16*, 6149–6159. [[CrossRef](#)]
7. Al-Sayyab, A.K.; Al Tmari, Z.Y.; Taher, M.K. Theoretical and experimental investigation of photovoltaic cell performance, with optimum tilted angle: Basra city case study. *Case Stud. Therm. Eng.* **2019**, *14*, 100421. [[CrossRef](#)]

8. Bailek, N.; Bouchouicha, K.; Aoun, N.; Mohamed, E.S.; Jamil, B.; Mostafaeipour, A. Optimized fixed tilt for incident solar energy maximization on flat surfaces located in the Algerian Big South. *Sustain. Energy Technol. Assess.* **2018**, *28*, 96–102. [[CrossRef](#)]
9. Wang, X.; Gao, X.; Wu, Y. Comprehensive analysis of tropical rooftop PV project: A case study in nanning. *Heliyon* **2023**, *9*, e14131. [[CrossRef](#)]
10. Kaddoura, T.O.; Ramli, M.A.; Al-Turki, Y.A. On the estimation of the optimum tilt angle of PV panel in Saudi Arabia. *Renew. Sustain. Energy Rev.* **2016**, *65*, 626–634. [[CrossRef](#)]
11. Despotovic, M.; Nedic, V. Comparison of optimum tilt angles of solar collectors determined at yearly; seasonal and monthly levels. *Energy Convers. Manag.* **2015**, *97*, 121–131. [[CrossRef](#)]
12. Jafarkazemi, F.; Saadabadi, S.A. Optimum tilt angle and orientation of solar surfaces in Abu Dhabi; UAE. *Renew. Energy* **2013**, *56*, 44–49. [[CrossRef](#)]
13. Chang, Y.P. Optimal the tilt angles for photovoltaic modules using PSO method with nonlinear time-varying evolution. *Energy* **2010**, *35*, 1954–1963. [[CrossRef](#)]
14. Khorasanizadeh, H.; Mohammadi, K.; Mostafaeipour, A. Establishing a diffuse solar radiation model for determining the optimum tilt angle of solar surfaces in Tabass; Iran. *Energy Convers. Manag.* **2014**, *78*, 805–814. [[CrossRef](#)]
15. Bojić, M.; Bigot, D.; Miranville, F.; Parvedy-Patou, A.; Radulović, J. Optimizing performances of photovoltaics in Reunion Island—Tilt angle. *Prog. Photovolt. Res. Appl.* **2012**, *20*, 923–935. [[CrossRef](#)]
16. Kaldellis, J.; Zafirakis, D. Experimental investigation of the optimum photovoltaic panels' tilt angle during the summer period. *Energy* **2012**, *38*, 305–314. [[CrossRef](#)]
17. Yan, R.; Saha, T.K.; Meredith, P.; Goodwin, S. Analysis of yearlong performance of differently tilted photovoltaic systems in Brisbane; Australia. *Energy Convers. Manag.* **2013**, *74*, 102–108. [[CrossRef](#)]
18. Gökmen, N.; Hu, W.; Hou, P.; Chen, Z.; Sera, D.; Spataru, S. Investigation of wind speed cooling effect on PV panels in windy locations. *Renew. Energy* **2016**, *90*, 283–290. [[CrossRef](#)]
19. Mehdi, M.; Ammari, N.; Merrouni, A.A.; Benazzouz, A.; Dahmani, M. Experimental investigation on the effect of wind as a natural cooling agent for photovoltaic power plants in desert locations. *Case Stud. Therm. Eng.* **2023**, *47*, 103038. [[CrossRef](#)]
20. Armstrong, S.; Hurley, W.G. A new methodology to optimise solar energy extraction under cloudy conditions. *Renew. Energy* **2010**, *35*, 780–787. [[CrossRef](#)]
21. N'Tsoukpoe, K.E. Effect of orientation and tilt angles of solar collectors on their performance: Analysis of the relevance of general recommendations in the West and Central African context. *Sci. Afr.* **2022**, *15*, e01069. [[CrossRef](#)]
22. Abdelaal, A.K.; El-Fergany, A. Estimation of optimal tilt angles for photovoltaic panels in Egypt with experimental verifications. *Sci. Rep.* **2023**, *13*, 3268. [[CrossRef](#)]
23. Teyabeen, A.A.; Mohamed, F. Modelling and Estimation of The Optimum Tilt Angle of Photovoltaic Systems; Case Study: Libya. In Proceedings of the 2022 13th International Renewable Energy Congress (IREC), Hammamet, Tunisia, 13–15 December 2022.
24. Nfaoui, M.; El-Hami, K. Extracting the maximum energy from solar panels. *Energy Rep.* **2018**, *4*, 536–545. [[CrossRef](#)]
25. Karinka, S.; Upadhyaya, V. Concept of annual solar window and simple calculation for optimal monthly tilt angle to maximize solar power generation. *Mater. Today Proc.* **2022**, *52*, 2166–2171. [[CrossRef](#)]
26. Prunier, Y.; Chuet, D.; Nicolay, S.; Hamon, G.; Darnon, M. Optimization of photovoltaic panel tilt angle for short periods of time or multiple reorientations. *Energy Convers. Manag. X* **2023**, *20*, 100417. [[CrossRef](#)]
27. Mamun, M.A.; Islam, M.M.; Hasanuzzaman, M.; Selvaraj, J. Effect of tilt angle on the performance and electrical parameters of a PV module: Comparative indoor and outdoor experimental investigation. *Energy Built Environ.* **2022**, *3*, 278–290. [[CrossRef](#)]
28. Awad, H.; Salim, K.E.; Gül, M. Multi-objective design of grid-tied solar photovoltaics for commercial flat rooftops using particle swarm optimization algorithm. *J. Build. Eng.* **2020**, *28*, 101080. [[CrossRef](#)]
29. Kornelakis, A. Multiobjective particle swarm optimization for the optimal design of photovoltaic grid-connected systems. *Sol. Energy* **2010**, *84*, 2022–2033. [[CrossRef](#)]
30. Shaddel, M.; Javan, D.S.; Baghernia, P. Estimation of hourly global solar irradiation on tilted absorbers from horizontal one using Artificial Neural Network for case study of Mashhad. *Renew. Sustain. Energy Rev.* **2016**, *53*, 59–67. [[CrossRef](#)]
31. Jeyaprabha, S.B.; Selvakumar, A.I. Optimal sizing of photovoltaic/battery/diesel based hybrid system and optimal tilting of solar array using the artificial intelligence for remote houses in India. *Energy Build.* **2015**, *96*, 40–52. [[CrossRef](#)]
32. Talebizadeh, P.; Mehrabian, M.A.; Abdolzadeh, M. Prediction of the optimum slope and surface azimuth angles using the Genetic Algorithm. *Energy Build.* **2011**, *43*, 2998–3005. [[CrossRef](#)]
33. Čongradac, V.; Prica, M.; Paspalj, M.; Bojanić, D.; Čapko, D. Algorithm for blinds control based on the optimization of blind tilt angle using a genetic algorithm and fuzzy logic. *Sol. Energy* **2012**, *86*, 2762–2770. [[CrossRef](#)]
34. Sangiorgio, S.; Sherwali, H.H.; Abufares, H.; Ashour, H. Investigation of optimum monthly tilt angles for photovoltaic panels in tripoli through solar radiation measurement. In Proceedings of the 2015 IEEE 15th International Conference on Environment and Electrical Engineering (EEEIC), Rome, Italy, 10–13 June 2015; pp. 565–569.
35. Mansour, F.A.; Nizam, M.; Anwar, M. Prediction of the optimum surface orientation angles to achieve maximum solar radiation using Particle Swarm Optimization in Sabha City Libya. In *IOP Conference Series: Materials Science and Engineering 2017*; IOP Publishing: Bristol, UK, 2017.
36. Nassar, Y.F.; Hafez, A.A.; Belhaj, S.; Alsadi, S.Y.; Abdunnabi, M.J.; Belgasim, B.; Sbeta, M.N. A Generic Model for Optimum Tilt Angle of Flat-Plate Solar Harvesters for Middle East and North Africa Region. *Appl. Sol. Energy* **2022**, *58*, 800–812. [[CrossRef](#)]

37. Nassar, Y.F.; El-Khozondar, H.J.; Abouhmod, N.M.; Abubaker, A.A.; Ahmed, A.A.; Alsharif, A.; Khaleel, M.M.; Elnaggar, M.; El-Khozondar, R.J. Regression model for optimum solar collectors' tilt angles in Libya. In Proceedings of the 2023 8th International Engineering Conference on Renewable Energy & Sustainability (ieCRES), Gaza, Palestine, 6 March 2023; pp. 1–6.
38. Kipp & Zonen. Instruction Manual, CMP Series Pyranometer, CMA Series Albedometer. 2013. Available online: <https://www.kippzonen.com> (accessed on 28 September 2022).
39. Piri, J.; Shamshirband, S.; Petković, D.; Tong, C.W.; ur Rehman, M.H. Prediction of the solar radiation on the earth using support vector regression technique. *Infrared Phys. Technol.* **2015**, *68*, 179–185. [[CrossRef](#)]
40. Pereira, A.B.; Nova, N.V.; Galvani, E. Estimation of global solar radiation flux density in Brazil from a single measurement at solar noon. *Biosyst. Eng.* **2003**, *86*, 27–34. [[CrossRef](#)]
41. Fernández-Peruchena, C.M.; Gastón, M.; Sánchez, M.; García-Barberena, J.; Blanco, M.; Bernardos, A. MUS: A multiscale stochastic model for generating plausible meteorological years designed for multiyear solar energy yield simulations. *Sol. Energy* **2015**, *120*, 244–256. [[CrossRef](#)]
42. Obiakor, P.I.; Awachie, I.R. Solar radiation pattern at Awka, Nigeria. *Energy Convers. Manag.* **1989**, *29*, 83–87. [[CrossRef](#)]
43. Taşdemirolu, E.; Sever, R. Estimation of total solar radiation from bright sunshine hours in Turkey. *Energy* **1989**, *14*, 827–830. [[CrossRef](#)]
44. Esteves, A.; De Rosa, C. A simple method for correcting the solar radiation readings of a Robitzsch-type pyranometer. *Sol. Energy* **1989**, *42*, 9–13. [[CrossRef](#)]
45. Global Solar Atlas. Available online: <https://globalsolaratlas.info/download/libya> (accessed on 28 September 2022).
46. Duffie, J.A.; Beckman, W.A. *Solar Engineering of Thermal Processes*; John Wiley & Sons: Hoboken, NJ, USA, 2013.
47. Teyabeen, A.A.; Elhatmi, N.B.; Essnid, A.A.; Mohamed, F. Estimation of monthly global solar radiation over twelve major cities of Libya. *Energy Built Environ.* **2024**, *5*, 46–57. [[CrossRef](#)]
48. Danandeh, M.A. Solar irradiance estimation models and optimum tilt angle approaches: A comparative study. *Renew. Sustain. Energy Rev.* **2018**, *92*, 319–330. [[CrossRef](#)]
49. Zang, H.; Guo, M.; Wei, Z.; Sun, G. Determination of the optimal tilt angle of solar collectors for different climates of China. *Sustainability* **2016**, *8*, 654. [[CrossRef](#)]
50. Yadav, A.K.; Chandel, S.S. Tilt angle optimization to maximize incident solar radiation: A review. *Renew. Sustain. Energy Rev.* **2013**, *23*, 503–513. [[CrossRef](#)]
51. Ashetehe, A.A.; Gessesse, B.B.; Shewarega, F. A generalized approach for the determination of optimum tilt angle for solar photovoltaic modules with selected locations in Ethiopia as illustration examples. *Sci. Afr.* **2022**, *18*, e01433. [[CrossRef](#)]
52. Teyabeen, A.A.; Jwaid, A.E. Modelling, Validation, and Simulation of Solar Photovoltaic Modules. *Electrica* **2023**, *23*, 48–60. [[CrossRef](#)]
53. Sharma, A.; Kallioğlu, M.A.; Awasthi, A.; Chauhan, R.; Fekete, G.; Singh, T. Correlation formulation for optimum tilt angle for maximizing the solar radiation on solar collector in the Western Himalayan region. *Case Stud. Therm. Eng.* **2021**, *26*, 101185. [[CrossRef](#)]
54. Teyabeen, A.A.; Elhatmi, N.B.; Essnid, A.A.; Mohamed, F. Comparison of seven empirical models for estimating monthly global solar radiation,(case study: Libya). In Proceedings of the 2021 12th International Renewable Energy Congress (IREC), Hammamet, Tunisia, 26–28 October 2021; pp. 1–6.
55. Taylor, K.E. Summarizing multiple aspects of model performance in a single diagram. *J. Geophys. Res. Atmos.* **2001**, *106*, 7183–7192. [[CrossRef](#)]

Disclaimer/Publisher's Note: The statements, opinions and data contained in all publications are solely those of the individual author(s) and contributor(s) and not of MDPI and/or the editor(s). MDPI and/or the editor(s) disclaim responsibility for any injury to people or property resulting from any ideas, methods, instructions or products referred to in the content.